Available online at www.sciencedirect.com
SCIENCE DIRECT®
Journal of Sound and Vibration 270 (2004) 767–780
JOURNAL OF SOUND AND VIBRATION
www.elsevier.com/locate/jsvi

Initial conditions in frequency-domain analysis: the FEM applied to the scalar wave equation

W.J. Mansur[a,*], D. Soares Jr.[a], M.A.C. Ferro[b]

[a] *Department of Civil Engineering, COPPE/Federal University of Rio de Janeiro, CP 68506, CEP, Rio de Janeiro, RJ 21945-970, Brazil*

[b] *Department of Fortification and Construction Engineering, IME, Praça General Tibúrcio 80,CEP 22290-270, Praia Vermelha, Rio de Janeiro, RJ, Brazil*

Received 19 June 2002; accepted 2 February 2003

Abstract

The present paper describes a procedure to consider initial conditions in the frequency-domain analysis of continuous media discretized by the FEM. The frequency-domain formulation presented here is based on a standard DFT procedure, the FFT algorithm being employed to transform from time to the frequency domain and vice versa. The standard Galerkin finite element method (displacement model) is used to replace the original differential governing equation by an integral equation amenable to numerical solution. The scalar wave equation (one- and two-dimensional) is used to illustrate the proposed approach. At the end of the paper, examples of wave propagation for a taut string, a one-dimensional rod and a membrane are presented to illustrate the robustness of the formulation presented here.

1. Introduction

The structural engineer usually has to choose a suitable methodology when carrying out the design of structures subjected to dynamic loads. Modal or nodal co-ordinates are used according to the characteristics of the dynamic structural system under study, for example the latter is usually preferred when strong non-linearities occur [1–5]. When either modal or nodal co-ordinates apply, the former (with modal truncation) is usually a better choice as the analysis may become much more economical.

The design work of engineers involved in daily time-domain dynamic analyses of structures has been greatly facilitated by several commercial codes available which include a number of

*Corresponding author. Tel.: +55-21-280-993; fax: +55-21-280-9545.
E-mail addresses: webe@coc.ufrj.br (W.J. Mansur), ferro@taurus.ime.eb.br (M.A.C. Ferro).

0022-460X/03/$ - see front matter © 2003 Elsevier Ltd. All rights reserved.
doi:10.1016/S0022-460X(03)00256-6

strategies for linear and non-linear analyses, and have excellent pre- and post-processing modules which simplifies enormously the daily design activities (ANSYS, ABACUS, SAP2000 Plus, COSMOS, GTSTRUDL, etc.).

A great deal of dynamic analyses can equivalently be performed either in time- or in frequency-domain. In many cases however, frequency-domain approaches are more adequate, e.g., when the physical properties are frequency dependent, when optimal design requires the use of spectra, etc. [1,6–14]. Frequency- and time-domain approaches do not, in fact, compete against each other, rather they are complementary.

Non-zero initial conditions contributions are naturally computed in standard time-marching algorithms usually employed in FE step-by-step approaches, e.g., Central Differences, Newmark, Wilson theta, α-Method, etc. [3–5,15]. The same applies to time-domain FE or BE procedures based on convolution, where integral terms to compute initial conditions appear explicitly [1,2,16–23].

One serious limitation of frequency-domain approaches based on DFT/FFT algorithms consists of the difficulty of such procedures to deal with non-null initial conditions [1,2,6–9,16,23,24].

The present paper describes a pseudo-force approach to consider non-zero initial conditions in DFT/FFT-based frequency-domain formulations. Generalized functions are used to mathematically describe the pseudo-forces present in the formulation. The idea of expressing constants with help of generalized functions when transform techniques are used is well known [16,25,26]. However, the context and the methodology adopted in the present paper to consider initial conditions are quite unique. The subject has been studied previously by Veletsos and Ventura [27,28] (see also Ref. [29]) who presented very useful procedures to consider initial conditions for SDOF mechanical systems which can be used also to eliminate the need of extending analyses periods (see Ref. [10]). However, the procedures presented in Refs. [27,28] are just useful for methodologies that employ modal co-ordinates. Actually, Veletsos and Ventura [28] presented a general approach (referred to by them as 'solution from frequency response function'), which can be nicely used either in modal or nodal co-ordinate analyses; however, for the latter it requires the computation of the problem time-domain Green's function from known frequency-domain matrix transfer functions. Even for the powerful super computers available nowadays, this methodology can only be recommended for very simple mechanical/structural systems.

The approach presented in the present paper is quite general. It can be used either when modal or nodal co-ordinates, as well as any transform procedure, is employed (Fourier, Laplace, Wavelet, etc.); and it is quite efficient.

It is straightforward to apply the methodology discussed here to hybrid frequency–time-domain analyses (see Ref. [16]) where frequency dependent properties must be considered together with non-linear behavior. The approach presented here can be employed to establish a real time segmented procedure in modal co-ordinates, where the previous time–history is replaced by initial conditions at the beginning of each segment, thus eliminating the need for convolution before the initial time of the current segment (see Refs. [10,27] for approaches adequate to modal analyses).

One- and two-dimensional examples are studied here concerning the transverse vibration of a taut string and a membrane, and the longitudinal vibration of a rod, analytical and BEM solutions of which can be found in Refs. [17,18].

The starting point for the development of the formulation presented here is the paper by Mansur et al. [10], where initial conditions are considered for the analysis of the discrete

spring-dash pot-mass mechanical system by the ImFT [10] approach. Two important advances are reported here: (1) extension of the ideas presented by Mansur et al. [10] to procedures based on DFT/FFT approaches; (2) generalization of the methodology, so that it can be used by a FEM-based algorithm either in nodal or in modal co-ordinates approaches (the same approach can be followed by finite differences, finite volumes, boundary elements, etc.).

2. Basic equations

The study carried out here concerns one- and two-dimensional scalar wave propagation problems. Only homogeneous isotropic systems will be considered; however, application of the FEM to other more complex problems is trivial, e.g., non-homogeneous anisotropic elastic medium (see Refs. [3,4,15]).

The scalar wave equation for isotropic homogeneous medium reads

$$\rho \frac{\partial^2 u(\mathbf{x},t)}{\partial t^2} + \mu \frac{\partial u(\mathbf{x},t)}{\partial t} - \kappa \nabla^2 u(\mathbf{x},t) = S(\mathbf{x},t), \tag{1}$$

where ∇^2 is the Laplace operator, κ is the bulk modulus of elasticity, ρ is the density and μ is the viscous damping coefficient. $u(\mathbf{x},t)$ is the unknown, which for the taut string and the membrane case analyses is the transverse displacement and in the case of wave propagation in rods is the longitudinal displacement; in acoustics it represents either pressure or velocity potential. $S(\mathbf{x},t)$ is the source term acting upon the domain.

The undamped version of Eq. (1) is more frequently found in wave propagation texts [30–33] in the form

$$\nabla^2 u(\mathbf{x},t) - \frac{1}{c^2}\frac{\partial^2 u(\mathbf{x},t)}{\partial t^2} = s(\mathbf{x},t), \tag{2}$$

where the parameter c is the wave propagation velocity given by $c = (\kappa/\rho)^{1/2}$. The following initial conditions are known over the Ω domain:

$$u(\mathbf{x},0) = u_0(\mathbf{x}), \quad \frac{\partial u(\mathbf{x},0)}{\partial t} = \dot{u}(\mathbf{x},0) = v_0(\mathbf{x}). \tag{3}$$

Dirichlet and Neumann boundary conditions over the Γ boundary are given by

$$u(\mathbf{x},t) = \bar{u}(\mathbf{x},t) \;\; x \in \Gamma_u, \;\; p(\mathbf{x},t) = \nabla u(\mathbf{x},t)\cdot\mathbf{n} = \frac{\partial u(\mathbf{x},t)}{\partial \mathbf{n}} = \bar{p}(\mathbf{x},t), \;\; \mathbf{x} \in \Gamma_p, \tag{4}$$

where $\Gamma(\Gamma = \Gamma_u \cup \Gamma_p)$ is the boundary of the Ω domain and $\mathbf{n}$ is the unit outward vector normal to Γ.

3. DFT approach for finite element analysis

The weak form of the weighted residual Galerkin FEM statement for Eq. (1) reads:

$$\kappa \int_\Omega (\nabla W \cdot \nabla u)\mathrm{d}\Omega + \mu \int_\Omega (W\dot{u})\mathrm{d}\Omega + \rho \int_\Omega (W\ddot{u})\mathrm{d}\Omega = \int_\Omega (WS)\mathrm{d}\Omega + \int_{\Gamma_p} (W\bar{p})\mathrm{d}\Gamma_p, \tag{5}$$

where W are the weighting functions, equal to interpolation functions since the Galerkin approach is employed, and dots mean time derivatives. After the standard u-discretization FEM procedure is introduced, Eq. (5) gives rise to [3,4,15]

$$\mathbf{M}\ddot{\mathbf{u}}(t) + \mathbf{C}\dot{\mathbf{u}}(t) + \mathbf{K}\mathbf{u}(t) = \mathbf{f}(t), \tag{6}$$

where $\ddot{\mathbf{u}}(t)$, $\dot{\mathbf{u}}(t)$ and $\mathbf{u}(t)$ are, respectively, nodal acceleration, velocity and displacement vectors; $\mathbf{f}(t)$ is the nodal equivalent force vector which accounts for contributions of body and surface forces; $\mathbf{M}$, $\mathbf{C}$ and $\mathbf{K}$ are mass, damping and stiffness matrices, respectively.

Initial conditions can be considered as pseudo-forces, in which case Eq. (6) can be written as

$$\mathbf{M}\Delta\ddot{\mathbf{u}}(t) + \mathbf{C}\Delta\dot{\mathbf{u}}(t) + \mathbf{K}\Delta\mathbf{u}(t) = \mathbf{r}(t), \tag{7}$$

where

$$\mathbf{r}(t) = \mathbf{f}(t) - \mathbf{f}_{\mathbf{U}_0}H(t-0) + \mathbf{f}_{\mathbf{V}_0}\delta(t-0), \tag{8}$$

$$\mathbf{f}_{\mathbf{U}_0} = \mathbf{K}\mathbf{u}_0, \quad \mathbf{f}_{\mathbf{v}_0} = \mathbf{M}\mathbf{v}_0 \tag{9, 10}$$

and $\Delta\mathbf{u}(t) = \mathbf{u}(t) - \mathbf{u_0}$; $\Delta\dot{\mathbf{u}}(t)$ and $\Delta\ddot{\mathbf{u}}(t)$ are, respectively, first (velocity) and second (acceleration) time derivatives of $\Delta\mathbf{u}(t)(\Delta\dot{\mathbf{u}}(t) = \dot{\mathbf{u}}(t)$ and $\Delta\ddot{\mathbf{u}}(t) = \ddot{\mathbf{u}}(t))$. $H(t-0)$ is the Heaviside function and $\delta(t-0)$ is the Dirac delta function. It should be observed that $\Delta\mathbf{u}(0) = 0$ and that the contribution of the initial velocity is taken into account by the pseudo-force vector given by Eq. (8).

The entries of the pseudo-force vector $\mathbf{f}_{\mathbf{U}_0}$, which accounts for the contributions of the initial displacements, are in fact nodal reactions due to $\mathbf{u}_0$ as it is indicated in Eq. (9) above. The pseudo-force vector $\mathbf{f}_{\mathbf{V}_0}$, on the other hand, is obtained in a way that one has the effect of the impulsive force $\mathbf{f}_{\mathbf{V}_0}\delta(t-0)$, indicated in Eq. (8), equal to the effect of the momentum variation due to the initial velocity vector $\mathbf{v}_0$ as shown by Eq. (10). $\mathbf{u_0}$ and $\mathbf{v_0}$ are the finite element nodal vectors whose entries are nodal values of the initial displacement and the initial velocity shown in Eq. (3).

Eq. (7) will be solved in the frequency-domain, so its Fourier transform has to be taken. The solution in the frequency-domain has to be obtained first and the inverse-Fourier transform carried out afterwards. Actually, a general approach cannot be analytical, thus the DFT and IDFT algorithms, illustrated, respectively, by expressions (11) and (12) below are used, where i is the imaginary unity, x_n are equally spaced time samples, i.e., x_n are elements of the discrete time series $\{x_n\}$, $n = 0,1,2,\ldots(N-1)$, and X_k are elements of the DFT of $\{x_n\}$ ($\{X_k\}$, $k = 0,1,2,\ldots(N-1)$, is the frequency spectrum)

$$X_k = \frac{1}{N}\sum_{n=0}^{N-1} x_n \exp\left(\frac{-2\pi \mathrm{i} kn}{N}\right), \quad k = 0, 1, 2, \ldots, (N-1), \tag{11}$$

$$x_n = \sum_{k=0}^{N-1} X_k \exp\left(\frac{-2\pi \mathrm{i} kn}{N}\right), \quad n = 0, 1, 2, \ldots, (N-1). \tag{12}$$

Each component of the solution spectrum is computed from the Fourier transform of Eqs. (7) and (8), i.e.

$$\Delta\mathbf{U}(\omega) = \mathbf{H}(\omega)\mathbf{R}(\omega) = \mathbf{H}(\omega)\{(FT[\mathbf{f}(t)]) - \mathbf{f}_{\mathbf{U}_0}(FT[H(t-0)]) + \mathbf{f}_{\mathbf{V}_0}(FT[\delta(t-0)])\}, \tag{13}$$

where $\Delta\mathbf{U}(\omega)$ and $\mathbf{R}(\omega)$ are the Fourier transforms of $\Delta\mathbf{u}(t)$ and $\mathbf{r}(t)$, respectively (FT$[\cdot]$ indicates Fourier transform), and $\mathbf{H}(\omega)$ is the frequency response transfer matrix, obtained from the inverse

of the impedance matrix $\mathbf{I}(\omega)$, given by

$$\mathbf{I}(\omega) = -\omega^2\mathbf{M} + \omega\mathrm{i}\mathbf{C} + \mathbf{K}. \tag{14}$$

It should be observed that in fact the inversion of the impedance matrix should be done only in very special cases; usually one can use Gauss triangularization reduction or else, iterative solvers which are computationally much more economical.

A modal approach can also be adopted [1–4,15]. By this procedure, assuming that the damping matrix is proportional, the transfer function matrix $\mathbf{H}^*(\omega)$, which correlates modal forces and the modal displacements, becomes diagonal, reducing considerably the analyses computational cost. $\mathbf{H}^*(\omega)$ can then be obtained from the inverse of the impedance matrix $\mathbf{I}^*(\omega)$, given by

$$\mathbf{I}^*(\omega) = \mathbf{diag}[-\omega^2 + 2\xi_j w_j \omega\mathrm{i} + w_j^2], \tag{15}$$

where $\mathbf{diag}[\cdot]$ means diagonal matrix, w_j is the jth natural frequency of the system and ξ_j is the damping ratio of the jth mode (as mentioned before i is the imaginary unit).

It is important to notice that $FT\{\delta(t-0)\}$ indicated in Eq. (13) can be obtained as

$$FT\{\delta(t-0)\} = D\{\int_{-\infty}^{+\infty} \delta(t-0)\mathrm{e}^{\mathrm{i}\omega t}\,\mathrm{d}t\} = D\{1\} = D = \frac{1}{N\Delta t} \tag{16}$$

as in the present case $D = 1/T_p$ where the extended period $T_p = N\Delta t$, Δt being the sampling time interval.

One last remark, which is due concerns the pseudo-force $\mathbf{f}_{\mathbf{U}_0}(FT[H(t-0)])$ used in Eq. (13) to compute contributions from the initial displacement field. Due to the periodicity of Fourier transform-based numerical algorithms, Heaviside functions cannot be considered acting during the whole extended period: the DFT algorithm will not consider the Heaviside function jump which occurs at $t = 0$, rather, the algorithm sees $H(t-0)$ as constant unit force acting from $-\infty$ to $+\infty$. The way to overcome this difficulty, which is inherent to DFT/FFT algorithms, is to consider the extended period T_p to be twice as long as that required by usual estimatives concerning short duration loads and keep $\mathbf{f}_{\mathbf{U}_0}$ constant from the initial time ($t = 0$) to T_p and make it null from time T_p to $2T_p$. The necessity to consider the time of the analysis equal to $2T_p$ instead of T_p makes the DFT/FFT algorithm more expensive when initial displacements contributions have to be computed than when initial velocities are present in the analysis, as the former has to be considered as a long duration load whereas the latter has the effect of a short duration one. However, it is important to observe that if the externally applied loads are of long duration, an extended period length larger than T_p will have to be considered anyway, thus the inclusion of the initial displacement contribution will not increase the computational cost.

4. Additional remarks concerning the dynamic equilibrium equations

This section presents a complementary discussion concerning the derivations leading from Eqs. (5) to (10). Standard FEM procedures [3–5] were followed; the unusual about the developments presented in Section 3 concerns considering contributions of initial displacement and initial velocity, explicitly, via the pseudo-forces equivalent nodal vectors $\mathbf{f}_{\mathbf{u}_0}\mathbf{H}(t-0)$ and $\mathbf{f}_{\mathbf{v}_0}\delta(t-0)$, respectively.

The pseudo-force vector $\mathbf{f}_{\mathbf{v}_0}\delta(t-0)$, whose contribution is equivalent to that of the initial velocity $v_0(x)$, can be determined from the momentum principle, a basic postulate of continuum mechanics, which quoting Malvern [34] can be described as: "the time rate of change of the total momentum of a given set of particles equals the vector sum of all the external forces acting on the particles of the set, provided Newton's third law of action and reaction governs the internal forces". Thus the contribution of the change in momentum from $t=0$ to 0^+ can be computed via a pseudo-body force $f_{v_0}(x,t)$ per unit volume such that the equation 'impulse = momentum change' is verified, i.e.

$$\int_{\Omega'}\left(\int_0^{0^+} f_{v_0}(x,t)\,\mathrm{d}t\right)\mathrm{d}\Omega' = \int_{\Omega'}\rho v_0(x)\mathrm{d}\Omega'. \tag{17}$$

The identity shown above must be satisfied for any arbitrarily chosen Ω' subdomain ($\Omega'\in\Omega$), thus

$$f_{v_0}(x,t) = \rho v_0(x)\delta(t-0). \tag{18}$$

When the pseudo-body force $f_{v_0}(x,t)$ is included on the right hand side of Eq. (5) the following additional integral has to be computed

$$\left\{\rho\int_\Omega W v_0(x)\,\mathrm{d}\Omega\right\}\delta(t-0). \tag{19}$$

Considering that the space interpolation for $v_0(x)$ is the same as that for $\ddot{u}(t)$ (which as usual in finite elements formulations is the same as that of $u(x,t)$), the result of the integral indicated in Eq. (19) is

$$\mathbf{M}\mathbf{v}_0\delta(t-0), \tag{20}$$

i.e., Eq. (10) is demonstrated. It should be observed that the derivation which transformed Eq. (19) into Eq. (20) followed the same steps required to transform the third integral on the left hand side of Eq. (5) into the matrix product indicated by the first term on the left hand side of Eq. (6).

The pseudo-force vector $\mathbf{f}_{\mathbf{u}_0}$ can be obtained when the following is considered:

$$u(x,t) = u_0(x) + \Delta u(x,t),\quad \dot{u}(x,t) = \Delta\dot{u}(x,t),\quad \ddot{u}(x,t) = \Delta\ddot{u}(x,t). \tag{21}$$

Thus, Eq. (6) can be written as

$$\mathbf{M}\Delta\ddot{\mathbf{u}} + \mathbf{C}\Delta\dot{\mathbf{u}} + \mathbf{K}(\mathbf{u}_0 + \Delta\mathbf{u}) = \mathbf{f}(t). \tag{22}$$

If one adds $-\mathbf{k}\mathbf{u}_0 H(t-0)$ to both sides of Eq. (22) it can finally be written as

$$\mathbf{M}\Delta\ddot{\mathbf{u}} + \mathbf{C}\Delta\dot{\mathbf{u}} + \mathbf{K}\Delta\mathbf{u} = \mathbf{r}(t) - \mathbf{K}\mathbf{u}_0 H(t-0). \tag{23}$$

Eqs. (23) and (20) demonstrate the result presented in Eq. (8).

It should be observed that the procedure described above concerning the pseudo-force vector $\mathbf{f}_{\mathbf{u}_0}$ leads to a physical interpretation where one can consider that the dynamical system was maintained at its initial displacement configuration by pseudo-forces $\mathbf{f}_{\mathbf{u}_0} = \mathbf{k}\mathbf{u}_0$for $t(-\infty, 0)$, and that at $t=0$ these pseudo-forces were canceled by the new applied forces $-\mathbf{k}\mathbf{u}_0 H(t-0)$.

5. Numerical examples

5.1. Preliminary remarks

In all the examples presented here, results obtained with the DFT approach were compared against those obtained with time-domain algorithms in order to check the accuracy of the procedure proposed here to consider non-null initial conditions in frequency-domain analyses. The time-domain results of example 1 were obtained using the computer code presented by Cooper [35] based on a time-domain finite difference procedure. Both time- and frequency-domain analyses of example 1 were performed in nodal co-ordinates, whereas examples 2 and 3 employed modal co-ordinates for both time- and frequency-domain analyses. Time-domain results presented in examples 2 and 3 were obtained using a standard Galerkin finite element method approach based on the Newmark time-marching algorithm, the trapezoidal rule as described by Bathe [3], Hughes [15], Zienkiewicz and Taylor [4] being used. The same time step 'length' Δt was adopted for both time- and frequency-domain analyses; however, the number of sampling points (N) adopted for the latter was greater than that for the former, as the extended period must be twice as large as the usual when initial displacement is considered. Linear finite elements were used in all the analyses presented here. The CST element was employed in the two-dimensional analyses; the one-dimensional FE approach employed a taut string element, mass and stiffness matrices being quite similar to those of truss elements in local co-ordinates.

5.2. Example 1

This example deals with the analysis of a taut string, which is fixed at its extremities and is subjected to prescribed initial velocity and displacement over its entire length. No external load is applied. The string characteristics are: $L = 10.0\,\mathrm{m}$ (length); $c = 1.0\,\mathrm{m/s}$ (wave propagation velocity); a viscous damping constant such that $\zeta = \mu/k = 0.10\,\mathrm{s/m^2}$(see Eq. (1)) was employed in the time- and frequency-domain analyses carried out in this example. The initial conditions adopted here are given by initial velocity: $v_0(x) = A_1 \sin(\pi x/L)$; initial displacement: $u_0(x) = A_2 \sin(\pi x/L)$; where for the present analysis: $A_1 = 10^{-3}\,\mathrm{m/s}$ and $A_2 = 10^{-3}\,\mathrm{m}$.

The natural frequencies can be easily obtained for this string model. The fundamental frequency (which is dominant) for instance is given by $w_0 = \pi c L^{-1}$ and as a consequence an extended period can be estimated by: $T_p = \alpha L \ln(10)/(\xi \pi c) = 0.733\alpha L/(\xi c)$, where $\xi = \zeta c/2\pi = 0.01592$. Adopting $\alpha = 2.75$ (see Ref. [10]) one has for the present case: $2T_p = 2533\,\mathrm{s}$. Taking this T_p estimation into consideration, the discretization parameters considered for the model were: $\Delta t = 1.0\,\mathrm{s}$, $2T_p = 4096\,\mathrm{s}$ and $N = 2^{12} = 4096$. Twenty linear elements were used for the one-dimensional finite element mesh.

The string displacement time–history is shown in Fig. 1. Fig. 1(a) shows the results for the model submitted to initial displacement only. The results depicted in Fig. 1(b) are due to initial velocity only.

5.3. Example 2

In this example the rod shown in Fig. 2 is analyzed. The domain and the boundary of this example are such that this two-dimensional analysis in fact reproduces classical one-dimensional

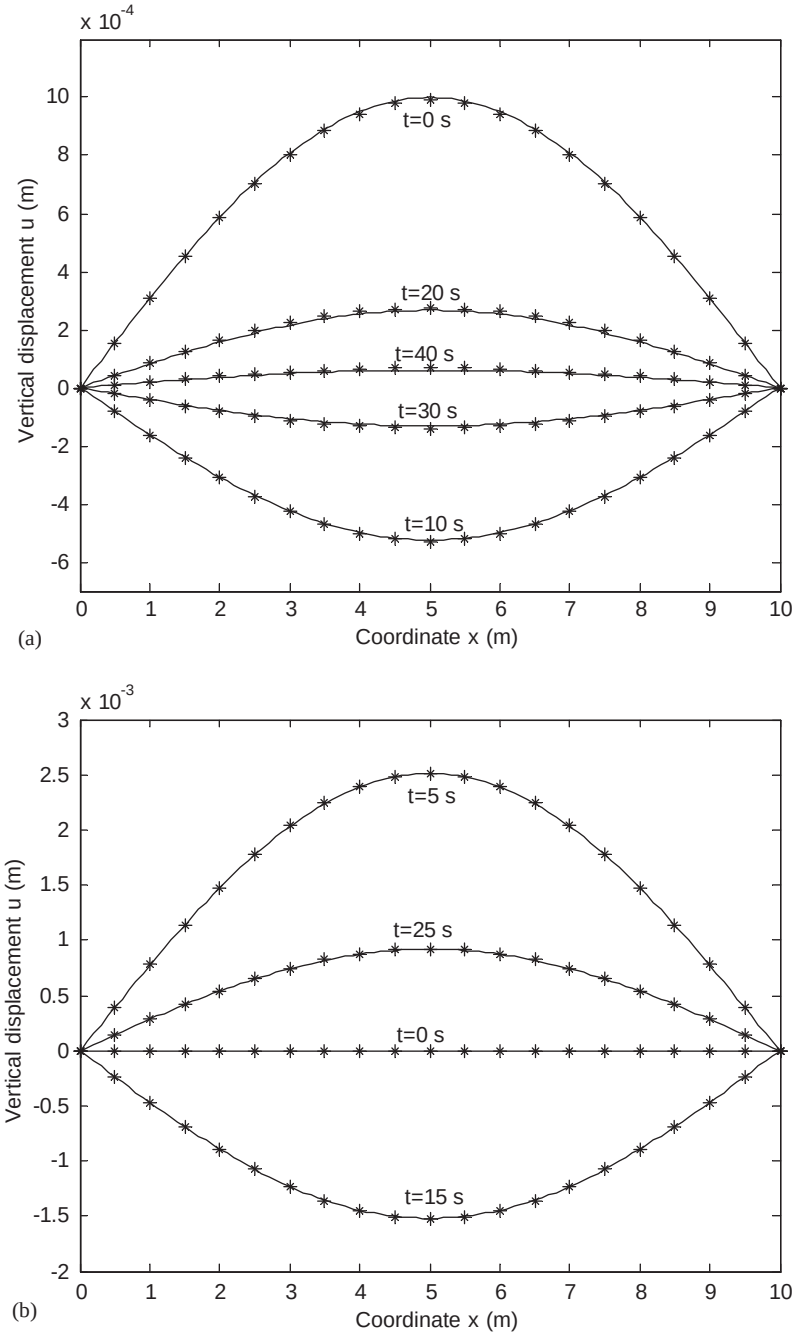

Fig. 1. Snap shots of the taut string. (a) Prescribed initial displacement; (b) prescribed initial velocity. ⁎, present method; —, Cooper [35].

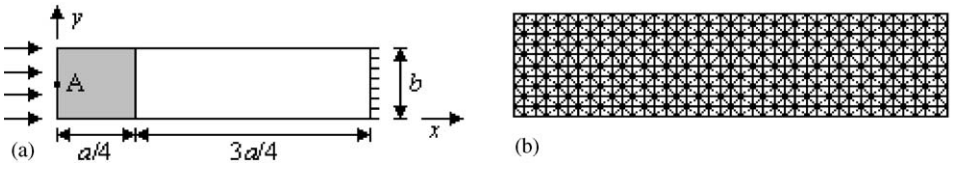

Fig. 2. Rod model: (a) boundary conditions and geometry definitions; (b) 2D finite element mesh.

rod results, as previously described by Mansur [17] and Mansur et al. [18]. The rod (see Fig. 2(a)) is fixed on its r.h.s. vertical boundary part, Γ_a , located at $x = a$, and has natural boundary conditions over its horizontal parts $\Gamma_b(y = b)$, $\Gamma_c(y = 0)$ and over its vertical boundary part Γ_0 defined by $x = 0$.

In the first analysis (case 1) the rod is excited by an uniform external load $p(x, t) = PH(t - 0)$, suddenly applied on Γ_a and kept constant until the end of the analysis. Initial conditions over the domain and surface forces on Γ_b and Γ_c are null. The rod is modelled by a bi-dimensional finite element mesh with 800 linear triangular elements as shown in Fig. 2(b).

The second analysis (case 2) considers boundary conditions identical to those of the first analysis, however the rod now is subjected to initial displacement and velocity, prescribed over the shaded area Ω_0 indicated in Fig. 2(a), expressed by

$$u_0(x, y) = \frac{P}{E}\left(\frac{a}{4} - x\right)\left\{1 - H\left(x - \frac{a}{4}\right)\right\},$$
$$v_0(x, y) = \frac{Pc}{E}\left\{1 - H\left(x - \frac{a}{4}\right)\right\},$$

where E is Young's modulus. When damping is not considered, the solution for this second analysis is the same as that of case 1, but with the time dephased by $(a/4c)$, i.e., $u'(x, y, t) = u\left(x, y, t - a/4c\right)$, where u' refers to case 1 and u refers to case 2. Similar relations hold for stresses, velocities, strains, surface tractions, etc.

The following numerical values were adopted for this analysis: $a = 1.00\,\text{m}$ (length) and $b = 0.25\,\text{m}$ (height); $c = 100\,\text{m/s}$ (wave propagation velocity); $\xi = 6.5\%$ (viscous damping ratio); and $P/E = 0.01$. The tolerance parameter (see Ref. [10]) considered for this rod analysis was $\alpha = 3.50$, which resulted in an extended period $2T_p = 1.58\,\text{s}$. The time discretization parameters adopted for the frequency-domain analyses were $\Delta t = 5 \times 10^{-5}\,\text{s}$ and $N = 2^{15}$.

As $u_0(x, y)$ is independent of the y co-ordinate, and varies linearly with x, within [0,a/4], the nodal force $\mathbf{f}_{U_0}$ equivalent to $u_0(x, y)$ are zero all over Ω_0, and not null on $x = 0$ and $a/4$; i.e., the effect of $u_0(x, y)$ in this case is equivalent to that of two body sources of intensity $p(x, y) = ktg\theta = k(4u_0(0, y)/a)$, suddenly applied at $t = 0$, and distributed over the vertical lines $x = 0$ and $a/4$, as illustrated in Fig. 3(a). Fig. 3(b) illustrates the equivalent load which simulates initial velocities.

The results obtained for the two analyses carried out here (labeled case 1 and case 2 as mentioned above) are depicted in Fig. 4. The time-domain FEM result for the undamped model, also displayed in Fig. 4, is quite close to the analytical solution (see Refs. [17,18]) and can be used as such for all practical purposes. Fig. 4 shows the excellent agreement between time- and frequency-domain approaches for both, cases 1 and 2; results are very close. The comparison of

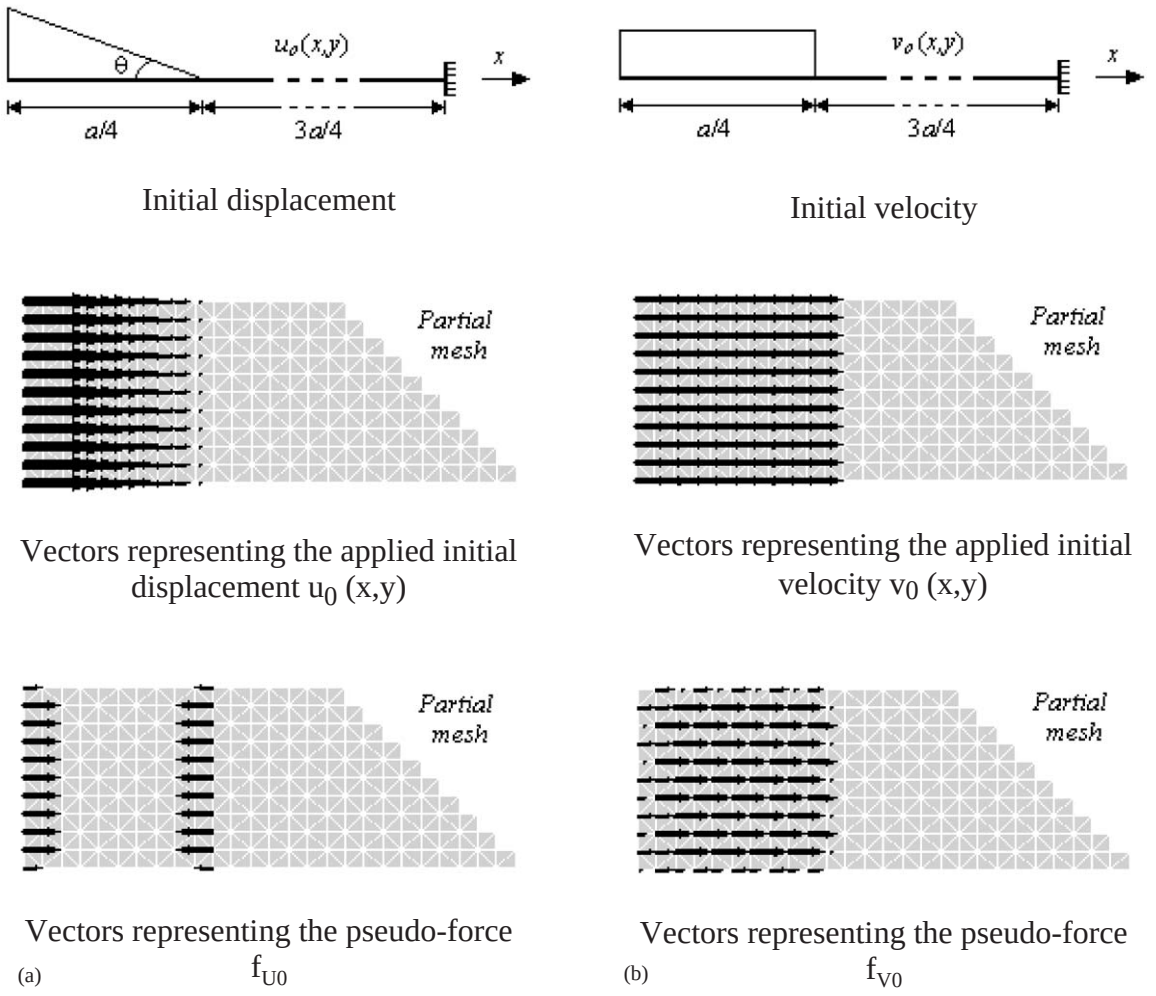

Fig. 3. Initial conditions and equivalent pseudo-forces: (a) nodal pseudo-load vector $\mathbf{f}_{\mathbf{u}_0}$ null everywhere except at $x = 0$ and $a/4$; (b) initial velocity replaced by the pseudo-load vector $\mathbf{f}_{v_0}$.

cases 1 and 2 responses also show that the $a/4c$ phase difference is accurately represented; thus the approach proposed here is also accurate in what concerns time shifting.

5.4. Example 3

The subject of this investigation is the transverse motion of a square membrane (see Ref. [17]) with initial velocity $v_0(x, y) = c$ prescribed over the shaded domain Ω_0 depicted in Fig. 5(a) and zero displacements prescribed over all the Γ boundary. The finite element mesh adopted can be seen in Fig. 5(b), where the transverse motion obtained for the membrane at time $t = 1.50$ s is depicted. Five thousand linear triangular elements were used in the mesh.

The displacement time–history at the center point of the membrane (point A, see Fig. 5(a)) is shown in Fig. 6. The numerical values for this analysis parameters were: $a = 1.0$ m; $c = 1.0$ m/s

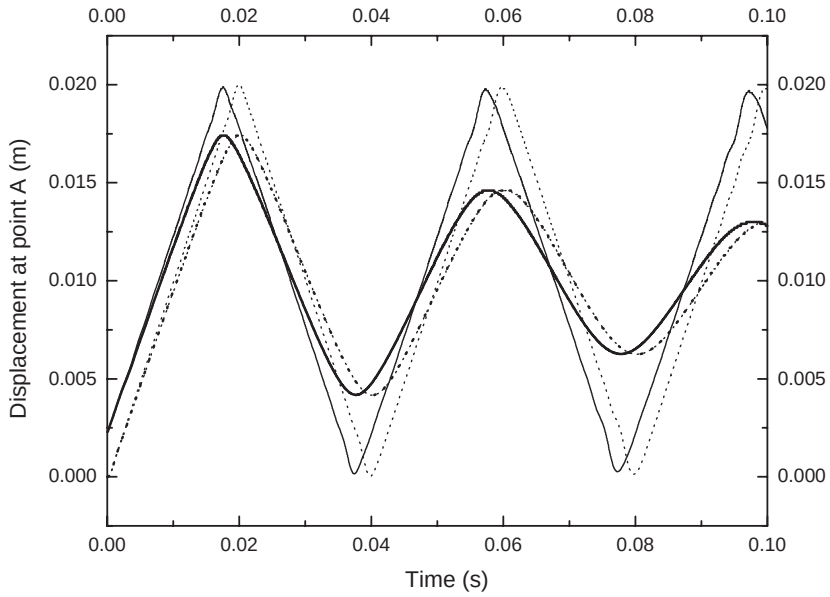

Fig. 4. Displacement time–history at point A (0, $b/2$). Case 1: rod under a Heaviside type forcing function; case 2: rod under a Heaviside type forcing function and prescribed initial velocity and displacement: ——, case 2, damped frequency/time-domain analyses; ——, case 2, undamped time-domain analysis; ·–·–·–, case 1, damped frequency/time-domain analyses; ·····, case 1, undamped time-domain analysis.

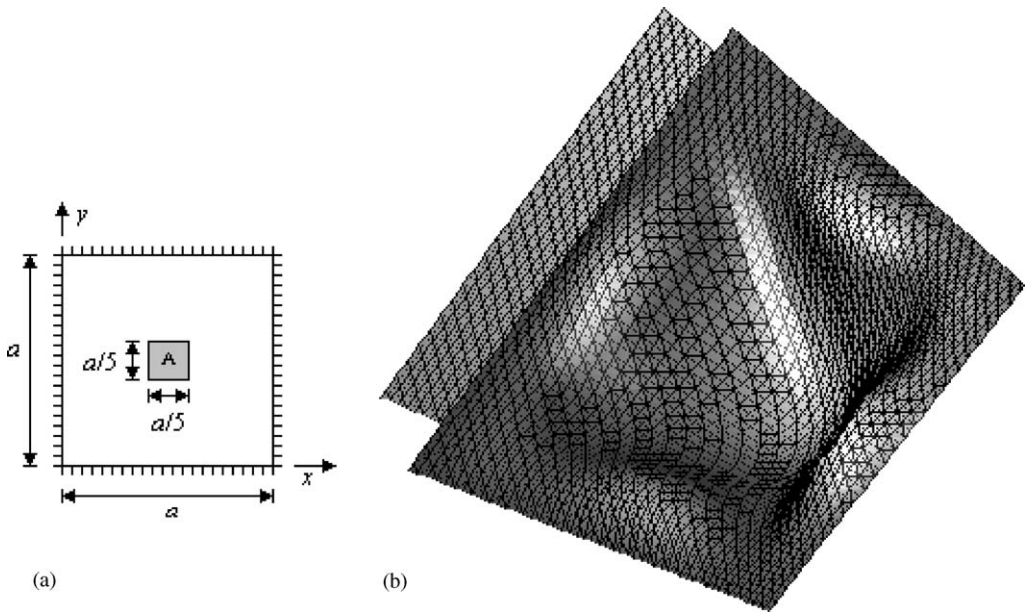

Fig. 5. Membrane analysis: (a) geometry definition, boundary and initial conditions; (b) finite element mesh representing the membrane transverse motion at time $t = 1.50$ s.

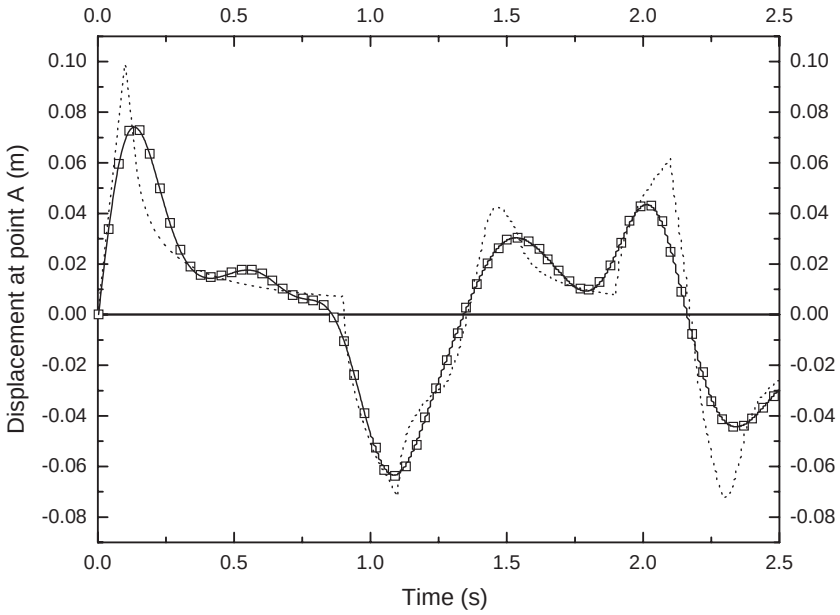

Fig. 6. Displacement time–history at point A ($a/2$, $a/2$) for the membrane analysis: □, damped frequency-domain analysis; ——, damped time-domain analysis; ·····, undamped analytical solution.

(wave propagation velocity); and $\xi = 2.5\%$ (viscous damping ratio). The membrane fundamental frequency is about $4.5\,s^{-1}$ and, as a consequence, by adopting $\alpha = 2.0$, the extended period can be estimated as $T_p = 41.0\,s$. The time interval and the number of sampling points considered for this analysis are, respectively, $\Delta t = 0.0025\,s$ and $N = 2^{14}$. The results obtained by frequency- (FFT) and time-domain (Newmark) procedures are quite close, so that their values plotted in Fig. 6 appear to coincide. The analytical result for the undamped model is also shown in Fig. 6.

6. Conclusions

This paper has presented a new procedure for considering the effects of initial conditions in frequency-domain analyses of continua media discretized by the FEM. The procedure described is quite general and increases the range of applicability of frequency-domain approaches as it makes it possible to develop time segmented algorithms in which convolution integrals to consider previous time–history need not be computed, i.e., only the current analysis segment must be considered at each step.

Two main papers dealt with this subject previously, Veletsos and Ventura [27] and Mansur et al., [10]. The formulation discussed in Ref. [27] is very useful; however, its application is restricted to Fourier transform-based algorithms and modal co-ordinates. The approach presented in Ref. [27] can also be used in nodal co-ordinates but it is not practical, as it requires very time consuming computations of time-domain the Green functions. The approach presented in Ref. [10] is also restricted to modal co-ordinates and Fourier transform-based algorithms. In

fact, the formulation presented in Ref. [10] was specifically developed within the context of the so-called implicit Fourier transform formulation (ImFT).

The approach presented here is suitable either to nodal or modal co-ordinates analyses, can be extended to other numerical methods, e.g., boundary elements, finite differences, finite volumes etc., and also can be used with other transform approaches, e.g., Laplace, wavelets, etc.

One- and two-dimensional problems governed by the scalar wave equation were analyzed, and the results obtained were quite accurate. The approach discussed here can easily be extended to three-dimensional scalar wave propagation analysis, elastodynamics, poroelastodynamics, acoustics, soil- and fluid-structure interaction, and to many others areas of engineering.

Another important remark concerning the formulation presented here is that it renders possible to do non-linear analysis in the frequency-domain, where only the current analysis segment is considered.

Acknowledgements

This work was supported by Finep/ANP (CTPETRO 769), CNPq (CTPETRO 462304-0), PRONEX/MCT (210140) and CAPES.

References

[1] R.W. Clough, J. Penzien, Dynamics of Structures, 2nd Edition, McGraw-Hill, New York, 1993.
[2] M. Paz, Structural Dynamics—Theory and Computation, 4th Edition, Chapman and Hall, New York, 1997.
[3] K.J. Bathe, Finite Element Procedures, Prentice-Hall, New Jersey, 1996.
[4] O.C. Zienkiewicz, R.L. Taylor, The Finite Element Method, Vols. I and II, McGraw-Hill, London, 1989.
[5] W. Weaver Jr., P.R. Johnston, Structural Dynamics by Finite Elements, Prentice-Hall, New Jersey, 1987.
[6] D.E. Newland, An Introduction to Random Vibration, Spectral & Wavelet Analysis, 3rd Edition, Longman Scientific & Technical, New York, 1993.
[7] J.P. Wolf, Dynamic Soil-Structure-Interaction, Prentice-Hall, New Jersey, 1985.
[8] A.V. Oppenheim, R.W. Schafer, Discrete Time Signal Processing, Prentice-Hall, New Jersey, 1989.
[9] J.G. Proakis, D.G. Manolakis, Digital Signal Processing—Principles, Algorithms and Applications, 3rd Edition, Prentice-Hall, New Jersey, 1996.
[10] W.J. Mansur, W.G. Ferreira, A.M. Claret, F. Venancio-Filho, J.A.M. Carrer, Time-segmented frequency-domain analysis for non-linear multi-degree-of-freedom structural systems, Journal of Sound and Vibration 237 (2000) 458–475.
[11] J.A. Inaudi, J.M. Kelly, Linear hysteretic damping and the Hilbert transform, Journal of Engineering and Mechanical Division, American Society of Civil Engineers 121 (1995) 626–632.
[12] N. Makris, J. Zhang, Time-domain viscoelastic analysis of earth structures, Earthquake Engineering and Structural Dynamics 29 (2000) 745–768.
[13] A.S. Veletsos, Y.T. Wei, Lateral and rocking vibration of footings, Journal of the Soil Mechanics and Foundations Division 97 (1971) 1227–1248.
[14] F.E. Richart, R.D. Woods, J.R. Hall, Vibrations of Soil and Foundations, Prentice-Hall, New Jersey, 1970.
[15] T.J.R. Hughes, The Finite Element Method, Dover Publications, New York, 1987.
[16] J.P. Wolf, Soil-Structure-Interaction Analysis in Time Domain, Prentice-Hall, New Jersey, 1988.
[17] W.J. Mansur, A time-stepping technique to solve wave propagation problems using the boundary element method, Ph.D. Thesis, University of Southampton, England, 1983.

[18] W.J. Mansur, J.A.M. Carrer, E.F.N. Siqueira, Time discontinuous linear traction approximation in time-domain BEM scalar wave propagation analysis, International Journal for Numerical Methods Engineering 42 (1998) 667–683.
[19] G. Yu, W.J. Mansur, J.A.M. Carrer, S.T. Lie, A more stable scheme for BEM/FEM coupling applied to two-dimensional elastodynamics, Computers & Structures 19 (2001) 811–823.
[20] W.J. Mansur, J.A.M. Carrer, G. Yu, in: O. von Estorff (Ed.), Boundary Elements in Acoustics—Advances & Applications, Computational Mechanics Publications, England, 2000 (Chapter 4).
[21] H. Antes, O. von Estorff, Analysis of absorption effects on the dynamic response of dam reservoir systems by boundary element methods, Earthquake Engineering and Structural Dynamics 15 (1987) 1023–1036.
[22] D.E. Beskos, Boundary element methods in dynamic analysis—II, Applied Mechanic Review 50 (1997) 149–197.
[23] J. Dominguez, Boundary Elements in Dynamics, Computational Mechanics Publications-Elsevier Applied Science, Southampton, 1993.
[24] L.A. De Lacerda, L.C. Wrobel, W.J. Mansur, A boundary integral formulation for two-dimensional acoustic radiation in a subsonic uniform flow, Journal of the Acoustical Society of America 100 (1996) 98–107.
[25] R.N. Bracewell, The Fourier Transform and its Applications, 2nd Edition, McGraw-Hill International Editions, New York, 1986.
[26] N. Makris, Stiffness, flexibility, impedance, mobility and the hidden delta function, Journal of Engineering Mechanics, American Society of Civil Engineers 123 (1997) 1202–1208.
[27] A.S. Veletsos, C. Ventura, Dynamic analysis of structures by the DFT method, Journal of Structural Engineering American Society of Civil Engineers 111 (1985) 2625–2642.
[28] A.S. Veletsos, C. Ventura, Efficient analysis of dynamic response of linear systems, Earthquake Engineering and Structural Dynamics 12 (1984) 521–536.
[29] J.M. Meek, A.S. Veletsos, Dynamic analysis by extra fast Fourier transform, Journal of the Engineering Mechanics Division American Society of Civil Engineers 98 (1972) 367–384.
[30] K.F. Graff, Wave Motion in Elastic Solids, Dover Publications, New York, 1975.
[31] J.D. Achenbach, Wave Propagation in Elastic Solids, North-Holland Publishing Company, Amsterdam, London, 1973.
[32] A.C. Eringen, E.S. Suhubi, Elastodynamics, Vols. I and II, Academic Press, New York, San Francisco, London, 1975.
[33] P.M. Morse, H. Feshbach, Methods of Theoretical Physics, McGraw-Hill, New York, Toronto, London, 1953.
[34] L.E. Malvern, Introduction to the Mechanics of a Continuous Medium, Englewood Cliffs, New Jersey, 1969.
[35] J. Cooper, Introduction to Partial Differential Equations with Matlab, Birkhauses, Berlin, 1998.